Diffraction–attenuation resistant beams: their higher-order versions and finite-aperture generations

Michel Zamboni-Rached,* Leonardo A. Ambrósio, and Hugo E. Hernández-Figueroa

Department of Microwaves and Optics, School of Electrical and Computer Engineering, University of Campinas, Campinas SP, Brazil

*Corresponding author: mzamboni@dmo.fee.unicamp.br

Received 16 July 2010; accepted 19 August 2010;
posted 10 September 2010 (Doc. ID 131600); published 18 October 2010

Recently, a method for obtaining diffraction–attenuation resistant beams in absorbing media has been developed in terms of suitable superposition of ideal zero-order Bessel beams. In this work, we show that such beams keep their resistance to diffraction and absorption even when generated by finite apertures. Moreover, we shall extend the original method to allow a higher control over the transverse intensity profile of the beams. Although the method is developed for scalar fields, it can be applied to paraxial vector wave fields, as well. These new beams have many potential applications, such as in free-space optics, medical apparatus, remote sensing, and optical tweezers. © 2010 Optical Society of America

OCIS codes: 140.3300, 260.1960, 350.7420.

1. Introduction

About six years ago [1,2], an interesting method was developed that is capable of delivering beams (in nonabsorbing media) whose longitudinal intensity pattern (LIP) can be chosen in advance. This method, named "Frozen Waves," is based on the superposition of copropagating Bessel beams, all with the same frequency. This method has been further generalized [3], allowing us to model the LIP of propagating beams in absorbing media. As a particular case, diffraction–attenuation resistant beams were obtained, that is, beams capable of maintaining both the size and the intensity of their central spots for long distances compared to ordinary beams.

The method for absorbing media was developed from appropriate superpositions of ideal zero-order Bessel beams. This has two fundamental implications: (a) beams with an infinite power flux (due to the use of ideal Bessel beams), and (b) beams with a spotlike transversal profile (due to the use of zero-order Bessel beams).

We shall extend the above method so as to obtain more efficient control over the transversal intensity profile of such beams by adopting superposition of higher-order Bessel beams.

We will also show that diffraction–attenuation resistant beams can maintain their interesting characteristics even when generated by finite apertures, i.e., even when we transversely truncate the Bessel beams that compose the desired beams. This demonstrates that, once the generation scheme is chosen, be it with antennas (in microwaves and millimetric waves), holograms, or spatial light modulators (in optics), the resulting beam may possess characteristics analogous to those of the ideal case, at least until a certain field depth. Although the method is developed for scalar fields, it can be applied to electromagnetic waves in the paraxial regime, and we will elucidate this point. These new beam solutions have many potential applications in medicine, remote sensing, free-space optics, and optical tweezers.

0003-6935/10/305861-09$15.00/0

2. Outline of the Method: Ideal Diffraction–Attenuation Resistant Beams in Absorbing Media

In [3], Zamboni-Rached developed a method capable of furnishing, *in absorbing media*, beams that are resistant to the effects of diffraction and, more importantly, capable of assuming any previously chosen LIP, in $\rho = 0$, in the range $0 < z < L$. As a particular case, this method is capable of furnishing diffraction–attenuation resistant beams for long distances compared to ordinary beams. With "diffraction–attenuation resistant" we mean that the central spots of these new beams maintain their shapes and also their intensities while propagating along an absorbing medium.

Such a method is based on suitable superpositions of equal-frequency zero-order Bessel beams and the core idea is to take on an extreme level the self-reconstructing property of the nondiffracting waves [4–30]. The obtained beams possess (initial) transverse field distributions capable of reconstructing not only the shapes of the central spots, but also the intensities of these spots. This happens without active action of the medium, which continues absorbing energy in the same way. This section presents the method developed in [3] with more details and some new results.

In an absorbing media with a complex refractive index given by

$$n(\omega) = n_R(\omega) + in_I(\omega), \tag{1}$$

a zero-order Bessel beam can be written as

$$\psi = J_0[(k_{\rho R} + k_{\rho I})\rho] \exp(i\beta_R z) \exp(-\beta_I z) \exp(-i\omega t), \tag{2}$$

where $\beta_R + i\beta_I \equiv \beta$ and $k_{\rho R} + k_{\rho I} \equiv k_\rho$ are the (complex) longitudinal and transversal wavenumbers, respectively, with their real and imaginary parts being given by

$$\beta_R = \frac{n_R\omega}{c}\cos\theta, \qquad \beta_I = \frac{n_I\omega}{c}\cos\theta, \tag{3}$$

$$k_{\rho R} = \frac{n_R\omega}{c}\sin\theta, \qquad k_{\rho I} = \frac{n_I\omega}{c}\sin\theta, \tag{4}$$

where $0 \le \theta \le \pi/2$ is the axicon angle of the beam. Note that $k_\rho^2 = n^2\omega^2/c^2 - \beta^2$. One can clearly see that the Bessel beam in Eq. (2) suffers an exponential decay along the propagation direction "z," due to the term $\exp(-\beta_I z)$.

The absorption coefficient of a Bessel beam with an axicon angle θ is given by $\alpha_\theta = 2\beta_I = 2n_I\omega\cos\theta/c$, its penetration depth being $\delta_\theta = 1/\alpha_\theta = c/(2\omega n_I\cos\theta)$. It is interesting to note that, because the transverse wavenumber k_ρ is complex, the beam transverse profile decays as a Bessel function until $\rho \approx 1/2k_{\rho I}$, beyond which it will suffer an exponential growth. This physically undesirable behavior occurs because Eq. (2) represents an ideal Bessel beam that needs to be generated by an infinite aperture. This problem, however, is solved when the beam is transversely truncated, i.e., when we use finite apertures in its generation. In these cases, the exponential growth along the transverse direction (for $\rho > 1/2k_{\rho I}$) must cease for a given value of ρ, and when the radius R of this aperture is such that $R < 1/2k_{\rho I}$, this exponential growth does not even occur [3]. It is important to remember that the efficient generation of a Bessel beam [5,6] occurs when the aperture radius [31] is such that $R \gg 2.4/k_{\rho R}$.

From the two conditions for R mentioned above, one can show [3] that, in an absorbing medium, a Bessel beam generated by a finite aperture of radius R will possess acceptable characteristics when $n_R \gg n_I$, i.e., when the coefficient of absorption for a plane wave is such that $\alpha \ll 1/\lambda \to \delta \gg \lambda$, where λ is the considered wavelength and δ is the penetration depth.

All cases considered here must obey this condition.

Now that the basic characteristics of a Bessel beam in an absorbing medium are understood, let us present the method developed in [3]. The idea is to achieve, in an absorbing medium with a refractive index $n(\omega) = n_R(\omega) + in_I(\omega)$, an axially symmetric beam [32], $\Psi(\rho, z, t)$, whose LIP along the propagating axis (i.e., on $\rho = 0$) can be freely chosen in a range $0 \le z \le L$. Let us say that the desired intensity profile in this range is given by $|F(z)|^2$. To obtain a beam with such characteristics, the following solution is proposed:

$$\begin{aligned}\Psi(\rho, z, t) &= \sum_{m=-N}^{N} A_m J_0(k_{\rho_m}\rho) e^{i\beta_m z} e^{-i\omega t} \\ &= e^{-i\omega t} \sum_{m=-N}^{N} A_m J_0((k_{\rho R_m} \\ &\quad + ik_{\rho I_m})\rho) e^{i\beta_{R_m} z} e^{-\beta_{I_m} z},\end{aligned} \tag{5}$$

with

$$k_{\rho_m}^2 = n^2\frac{\omega^2}{c^2} - \beta_m^2, \tag{6}$$

which implies that

$$\frac{\beta_{R_m}}{\beta_{I_m}} = \frac{k_{\rho R_m}}{k_{\rho I_m}} = \frac{n_R}{n_I}, \tag{7}$$

where $\beta_m = \beta_{R_m} + i\beta_{I_m}$ and $k_{\rho_m} = k_{\rho R_m} + ik_{\rho I_m}$.

Equation (5) is a superposition of $2N + 1$ copropagating Bessel beams with the same angular frequency ω. In Eq. (5), the coefficients A_m, the longitudinal (β_m), and the transverse ($k_{\rho m}$) wavenumbers are yet to be determined. The choice of these values is made such that the desired result (i.e., $|\Psi(\rho = 0, z, t)|^2 = |F(z)|^2$ within $0 \le z \le L$) is obtained. The following choice is made:

$$\beta_{R_m} = Q + \frac{2\pi m}{L}, \tag{8}$$

where Q is a constant such that

$$0 \le Q + \frac{2\pi m}{L} \le n_R \frac{\omega}{c}, \tag{9}$$

for $-N \le m \le N$.

The condition in Eq. (9) ensures forward propagation only, with no evanescent waves. In Eq. (8) Q is a constant value that can be freely chosen, as long as Eq. (9) is obeyed, and it plays an important role in determining the spot size of the resulting beam (lower values of Q imply narrower spots), as we will show below. Additionally, Q can be chosen such as to guarantee the paraxial regime in an electromagnetic beam. In this case, Q must possess a value close to $n_R\omega/c$. We will see this in detail in Section 3.

With the choice of Eq. (8), the superposition of Eq. (5) is written as

$$\Psi(\rho,z,t) = e^{-i\omega t}e^{iQz}\sum_{m=-N}^{N} A_m J_0((k_{\rho R_m} + ik_{\rho I_m})\rho)e^{i\frac{2\pi m}{L}z}e^{-\beta_{I_m}z}, \tag{10}$$

where, by inserting Eq. (8) into Eq. (7),

$$\beta_{I_m} = \left(Q + \frac{2\pi m}{L}\right)\frac{n_I}{n_R}, \tag{11}$$

and $k_{\rho_m} = k_{\rho R_m} + ik_{\rho I_m}$ is obtained through Eq. (6).

The maxima and minima of the imaginary parts of the various β_{Im} are given by $(\beta_I)_{\min} = (Q - 2\pi N/L)\, n_I/n_R$ and $(\beta_I)_{\max} = (Q + 2\pi N/L)n_I/n_R$, and the central value (for $m = 0$) is given by $(\beta_I)_{m=0} = Qn_I/n_R \equiv \bar{\beta}_I$.

Now, let us consider the ratio

$$\Delta = \frac{(\beta_I)_{\max} - (\beta_I)_{\min}}{\bar{\beta}_I} = 4\pi\frac{N}{LQ}. \tag{12}$$

For $\Delta \ll 1$, there are no considerable numerical differences among the various β_{Im} and we can safely approximate them by $\beta_{I_m} \approx \bar{\beta}_I$, which implies that $\exp(-\beta_{I_m}z) \approx \exp(-\bar{\beta}_I z)$. In these cases, the series in Eq. (5) evaluated on $\rho = 0$ can be (approximately) considered a truncated Fourier series, multiplied by the function $\exp(-\bar{\beta}_I z)$. Therefore, this series can be used to reproduce the desired longitudinal profile $|F(z)|^2$ (on $\rho = 0$), within $0 \le z \le L$, as long as we make

$$A_m = \frac{1}{L}\int_0^L F(z)e^{\bar{\beta}_I z}e^{-i\frac{2\pi m}{L}z}dz. \tag{13}$$

Essentially, this is the method developed in [3]. It is interesting to note that countless beams with the same desired LIP, but with different values of the parameter Q, can be constructed. The basic difference among them will be their spot radius ($\Delta\rho$), which can be estimated as being

$$\Delta\rho \approx \frac{2.4}{k_{\rho R_{m=0}}} = \frac{2.4}{\sqrt{\frac{n_R^2\omega^2}{c^2} - Q^2}}. \tag{14}$$

So, besides choosing the desired LIP of the beam in an absorbing medium, we can stipulate its spot size. In Section 4 we will show that a more efficient control over the beam transverse intensity pattern is obtained by using higher-order Bessel beams in the superposition of Eq. (5).

In summary, we wish to obtain a propagating beam in an *absorbing medium* possessing, inside the interval $0 \le z \le L$, a previously chosen LIP (on $\rho = 0$) given by $|F(z)|^2$. To achieve such a profile, we write the desired beam as a superposition of $2N + 1$ copropagating Bessel beams [Eq. (5)] by suitably choosing the longitudinal ($\beta_m = \beta_{R_m} + i\beta_{I_m}$) and transverse ($k_{\rho_m} = k_{\rho R_m} + ik_{\rho I_m}$) wavenumbers, and the coefficients A_m according to Eqs. (8), (9), (11), (6), and (13). We can also stipulate the spot radius, $\Delta\rho$, of the beam through a suitable choice of the parameter Q in Eq. (14).

The method demonstrates to be efficient in situations where [33] $\alpha \ll 2/\lambda$ and $\Delta = 4\pi N/LQ \ll 1$, allowing us to obtain a great variety of beams with potentially interesting intensity profiles as, for example, beams capable of maintaining not only the size of their central spots, but also the intensity of these spots until a certain chosen distance along the absorbing medium in question. We can call these types of beams "diffraction–attenuation resistant beams."

We finish this section with an example [34] of the above-mentioned beam.

Example

Consider an absorbing medium with a refractive index $n = 1.5 + i0.49 \times 10^{-6}$ in $\lambda = 308\,\text{nm}$ (i.e., $\omega = 6.12 \times 10^{15}\,\text{Hz}$). In this bulk, at this angular frequency, we have the following behaviors for the following wave solutions: (a) a plane wave possesses a penetration depth of $\delta = 1/\alpha = c/(2\omega n_I) = 5\,\text{cm}$; (b) a Gaussian beam with initial spot of radius $5.6\,\mu\text{m}$, besides suffering attenuation, is also affected by a strong diffraction, having a diffraction length of only 0.6 mm; and (c) an ideal Bessel beam with a central spot of radius $5.6\,\mu\text{m}$ (which implies an axicon angle of 0.0141 rad) can maintain its spot size, but suffers attenuation, possessing a penetration depth of $\delta_\theta = 1/\alpha_\theta = c/(2\omega n_I \cos\theta) = 5\,\text{cm}$.

Now, we are going to use the method exposed in this section to obtain a beam with spot radius $\Delta\rho = 5.6\,\mu\text{m}$, capable of maintaining the size and the intensity of its central spot until a distance of 25 cm, i.e., a penetration depth 5 times greater than those of the Bessel beam and of the plane wave [35], and a diffractionless distance 100 times greater than that of the Gaussian beam. We also demand that the spot intensity suffers a strong fall after the distance $z = 25\,\text{cm}$.

This diffraction–attenuation resistant beam can be obtained through the solution of Eq. (5) by choosing the desired LIP $|F(z)|^2$ (on $\rho = 0$), within $0 \le z \le L$, according to

$$F(z) = \begin{cases} 1 & \text{for } 0 \le z \le Z \\ 0 & \text{elsewhere} \end{cases}, \tag{15}$$

putting $Z = 25\,\text{cm}$, with, for example, $L = 33\,\text{cm}$. The stipulated spot radius, $\Delta\rho = 5.6\,\mu\text{m}$, is obtained by putting $Q = 0.9999 n_R \omega/c$ in Eq. (14). This value of Q is used for the β_{R_m} in Eq. (8), and we choose $N = 20$ [36]. The values of β_{Im} and $k_{\rho m}$ are calculated from Eqs. (11) and (6), respectively. Finally, we use Eq. (13) to find the coefficients [37] A_m of Eq. (10), defining in this way the desired beam.

We can see that the resulting beam fits very well all the desired characteristics, as is shown in Fig. 1(a), which is the three-dimensional field-intensity, and in Fig. 1(b), which is the orthogonal projection in logarithmic scale. The resulting beam possesses a spot radius of $5.6\,\mu\text{m}$ and maintains the size and intensity of its central core until the desired distance of 25 cm, suffering after that an abrupt intensity fall.

As we will see in Section 5, the truncated version of this beam will maintain these characteristics if the radius R of the finite aperture used for truncation obeys $R \ge 3.8\,\text{mm}$. This is already suggested by Fig. 1(b), which shows the ideal (i.e., not truncated) beam.

3. Electromagnetic Beams: the Paraxial Regime

It should be clear to the reader that the present method is exact, i.e., the obtained beams (with the desired LIPs) in absorbing media are exact solutions to the scalar wave equation and can possess transverse spots of any sizes, from wavelength dimensions to infinity. Although the method has been developed for scalar fields, it can be used in electromagnetism (optics, microwaves, etc.) in the paraxial regime, where the scalar beam Ψ of Section 2 would represent the transverse Cartesian electric field component of a linearly polarized electromagnetic beam, $|\Psi|^2$ being proportional to the time-averaged electromagnetic energy density. In these cases, the beam spot size must be much greater than the corresponding wavelength. This can be done by choosing the parameter Q of Eq. (8) as $Q \approx n_R \omega/c$.

We are going to elucidate all these points.

Consider an absorbing, linear, homogeneous and isotropic medium without boundaries and without free charges and free currents. The electric (and magnetic) field obeys, in the monochromatic case, the Helmholtz equation:

$$\nabla^2 \mathbf{E} + k^2 \mathbf{E} = 0, \tag{16}$$

with $\mathbf{E} = \mathcal{E}(x,y,z)e^{-i\omega t}$, and where k is the complex wavenumber:

$$k = \frac{\omega}{c} n(\omega) = \omega\sqrt{\mu(\omega)\epsilon(\omega)} = \omega\sqrt{\mu\left(\epsilon_b + i\frac{\sigma}{\omega}\right)}, \tag{17}$$

where $\epsilon_b(\omega)$ is the electric permittivity due to bound electrons, $\sigma(\omega)$ is the electric conductivity, and $\mu \approx \mu_0$ is the magnetic permeability. Writing k as

$$k = k_R + ik_I, \tag{18}$$

and considering a frequency not so close to the resonance regions [38], we have [39]

$$k_R \approx \omega\sqrt{\frac{\mu_0\epsilon_b}{2}}\left[\sqrt{1 + \left(\frac{\sigma}{\epsilon_b\omega}\right)^2} + 1\right]^{1/2}, \tag{19}$$

$$k_I \approx \omega\sqrt{\frac{\mu_0\epsilon_b}{2}}\left[\sqrt{1 + \left(\frac{\sigma}{\epsilon_b\omega}\right)^2} - 1\right]^{1/2}, \tag{20}$$

with the absorption coefficient [40] $\alpha = 2k_I$.

Let $\mathbf{E}$ be an electric field given by

$$\mathbf{E} = E_x \mathbf{e}_x + E_z \mathbf{e}_z, \tag{21}$$

and let us apply our scalar method to the Cartesian component E_x:

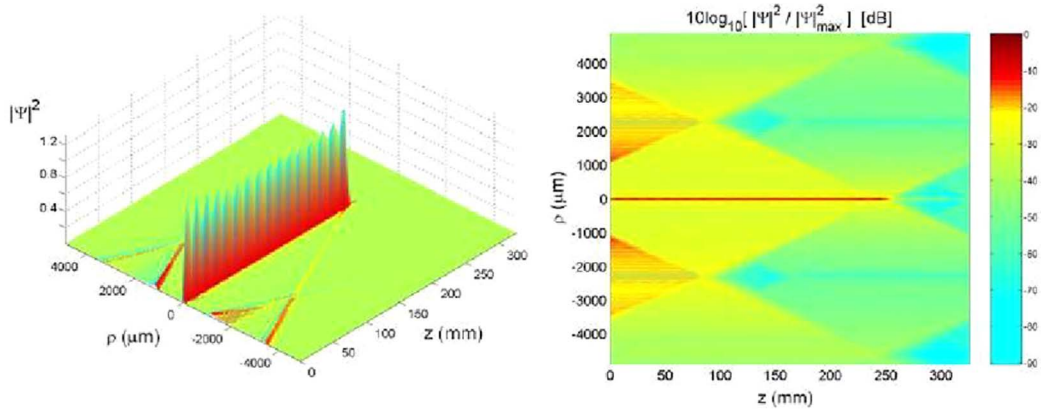

(a) (b)

Fig. 1. (Color online) (a) Three-dimensional field intensity of the resulting beam. (b) Orthogonal projection of the resulting beam intensity (normalized with respect to its maximum value, $|\Psi|^2_{\text{max}}$) in logarithmic scale.

$$E_x(\rho,z,t) = e^{-i\omega t}\sum_{m=-N}^{N} A_m J_0(k_{\rho m}\rho)e^{i\beta_m z}$$
$$= e^{-i\omega t}e^{iQz}\sum_{m=-N}^{N} A_m J_0((k_{\rho R_m} + ik_{\rho I_m})\rho)e^{-\beta_{I_m} z}e^{i\frac{2\pi}{L}mz}, \quad (22)$$

where, as before, $\beta_m = \beta_{R_m} + i\beta_{I_m}$ and $k_{\rho m} = k_{\rho R_m} + ik_{\rho I_m}$ are chosen according to Eqs. (8), (9), (11), and (6), and A_m is calculated through Eq. (13), with $|F(z)|^2$ as the desired LIP to the electric field component E_x. Now, to satisfy the Gauss law $\nabla\cdot\mathbf{D} = 0$ (no free charges), with $\mathbf{E} = E_x\mathbf{e}_x + E_z\mathbf{e}_z$, in the monochromatic regime, we must have

$$E_z = -\int \frac{\partial E_x}{\partial x}dz. \quad (23)$$

Using E_x as given by Eq. (22), we found

$$E_z(\rho,\phi,z,t) = e^{-i\omega t}\sum_{m=-N}^{N} A_m \frac{k_{\rho m}}{\beta_m}J_1(k_{\rho m}\rho)\cos\phi e^{i\beta_m z}. \quad (24)$$

The paraxial regime is characterized by beams in which the wave vectors of the constituent plane waves are almost parallel to their propagation directions. In our case, this direction is "$+z$" and the paraxial regime is reached by putting $Q \approx n_R\omega/c$, implying that $|k_{\rho m}/\beta_m| \ll 1$, which, in turn, implies that $|E_z| \ll |E_x|$. So, in this circumstance, we can use the so-called paraxial approximation and write the electric field in Eq. (21) as

$$\mathbf{E} \approx E_x\mathbf{e}_x = \left(e^{-i\omega t}\sum_{m=-N}^{N} A_m J_0(k_{\rho m}\rho)e^{i\beta_m z}\right)\mathbf{e}_x \quad (25)$$
$$(\textit{paraxial approximation}),$$

The associated magnetic field can be found through Faraday's law:

$$\mathbf{B} = -\frac{i}{\omega}\nabla\times\mathbf{E}. \quad (26)$$

Considering the electric field given by Eqs. (21), (22), and (24), it is easy to show that, in the paraxial regime, Eq. (26) can be approximated as

$$\mathbf{B} \approx -\frac{i}{\omega}\frac{\partial E_x}{\partial z}\mathbf{e}_y = \left(e^{-i\omega t}\sum_{m=-N}^{N} A_m \frac{\beta_m}{\omega}J_0(k_{\rho m}\rho)e^{i\beta_m z}\right)\mathbf{e}_y$$
$$(\textit{paraxial approximation}). \quad (27)$$

Remembering that $\beta_m = \beta_{R_m} + i\beta_{I_m} = \beta_{R_m} + i(n_I/n_R)\beta_{R_m}$, and that $0 \le \beta_{R_m} \le Q + 2\pi m/L$, the paraxial regime ($Q \approx n_R\omega/c$) implies that $\beta_{R_m} \approx n_R\omega/c$, and, in this case, $\beta_m/\omega \approx n/c$ (where $n = n_r + in_I$ is the complex refractive index). So, we can make another approximation in Eq. (27), writing

$$\mathbf{B} \approx \frac{n}{c}\left(e^{-i\omega t}\sum_{m=-N}^{N} A_m J_0(k_{\rho m}\rho)e^{i\beta_m z}\right)\mathbf{e}_y, \quad (28)$$

or

$$\mathbf{B} \approx \frac{n}{c}\mathbf{e}_z\times\mathbf{E} = \frac{n}{c}E_x\mathbf{e}_y \qquad (\textit{paraxial approximation}). \quad (29)$$

By using Eqs. (25) and (29), we immediately see that the time-averaged energy density for monochromatic electromagnetic fields, $u = (1/4)\mathrm{Re}(\mathbf{E}\cdot\mathbf{D}^* + \mathbf{B}\cdot\mathbf{H}^*)$, can be approximated as

$$u \approx \frac{1}{4}\mathrm{Re}\left(\epsilon^* + \frac{|n|^2}{\mu^* c^2}\right)|E_x|^2 \propto |E_x|^2 \quad (30)$$
$$(\textit{paraxial approximation}).$$

So, we can use our scalar method to obtain, in absorbing media, paraxial electromagnetic beams whose time-averaged energy densities on the propagation axis can assume any desired patterns within an interval $0 \le z \le L$.

4. Extending the Method to Nonaxially Symmetric Beams: Increasing the Control over the Transverse Intensity Pattern

The method developed in [3] allows strong control over the LIP (on $\rho = 0$) of beams propagating in absorbing media. Once we have controlled the beam's LIP, the transverse intensity pattern (TIP) can be shaped in a limited way; more specifically, the spot size of the resultant beam can be chosen by a suitable choice of the parameter Q via Eq. (14).

In this section [41], we are going to show that it is possible to get more efficient control over the TIP, maintaining, at the same time, strong control over the LIP. It will be possible, for instance, to shift the desired LIP from $\rho = 0$ to $\rho = \rho' > 0$. In other words, we will be able to construct the desired LIP over cylindrical surfaces (instead of over the line $\rho = 0$). Below we explain this new procedure.

To obtain these new beams, we proceed as before, choosing the desired LIP on $\rho = 0$ within $0 \le z \le L$, choosing the values of Q and N [observing Eq. (9)], and calculating the values of A_m through Eq. (13). Having done this, we replace the zero-order Bessel beams in the superposition of Eq. (10) with higher-order ones. The new beam is written as

$$\Psi(\rho,\phi,z,t) = e^{-i\omega t}e^{iQz}e^{i\mu\phi}\sum_{m=-N}^{N} A_m J_\mu(k_{\rho m}\rho)e^{-\beta_{I_m} z}e^{i\frac{2\pi}{L}mz}, \quad (31)$$

with μ as a positive integer, and all other parameters (Q, N, L, and A_m) given and calculated as before.

For the situations considered here, we have that $n_I \ll n_R \to k_{\rho I_m} \ll k_{\rho R_m}$. This implies that, for each Bessel function in Eq. (31), the following is valid: $J_\mu[(k_{\rho R_m} + ik_{\rho I_m})\rho] \approx J_\mu(k_{\rho R_m}\rho)$ for $0 < \rho \ll 1/k_{\rho I_m}$, and in this range each Bessel function reaches its maximum value at $\rho = \rho'_m$, ρ'_m being the first positive root of the equation $(\mathrm{d}J_\mu(k_{\rho R_m}\rho)/\mathrm{d}\rho)|_{\rho'_m} = 0$. The values of ρ'_m are located around the central value $\rho'_{m=0}$ and we can expect a shift of the desired LIP from $\rho = 0$ to $\rho \approx \rho'_{m=0}$.

We have confirmed this conjecture in all situations considered by us, mainly in the cases where there is no considerable difference among the values of $k_{\rho R_m}$. With this extension of the original method, it is possible to model the LIP over cylindrical surfaces, obtaining very interesting static configurations of the field intensity. In particular, we can construct hollow beams resistant to the attenuation and diffraction effects.

To illustrate this method, we are going to obtain a cylindrical light surface of constant intensity in an absorbing medium with $n_R = 1.5$ and $\alpha = 20\,\mathrm{m}^{-1}$ (at $\lambda = 308\,\mathrm{nm} \to \omega = 6.12 \times 10^{15}\,\mathrm{Hz}$), which implies that $n_I = 0.49 \times 10^{-6}$. At this angular frequency, an ordinary beam would possess a depth of penetration of 5 cm in this medium. Let us choose, within $0 \le z \le L$, a LIP as that in Section 2, Eq. (15):

$$F(z) = \begin{cases} 1 & \text{for } 0 \le z \le Z \\ 0 & \text{elsewhere} \end{cases}, \tag{32}$$

where $Z = 25\,\mathrm{cm}$ and $L = 33\,\mathrm{cm}$.

As in Section 2, we put $Q = 0.9999 n_R \omega/c$ in Eq. (8). With the chosen values of Q and L, the maximum value allowed for N is $N = 154$, but for simplicity we choose $N = 20$.

Using Eqs. (8), (9), (11), (6), and (13) we evaluate all the β_m, $k_{\rho m}$, and A_m. But, as we have explained in this section, instead of using all these values in Eq. (10), we use them in the superposition in Eq. (31), where we choose $\mu = 4$. According to the previous discussion, we can expect the desired LIP over a cylindrical surface of radius $\rho \approx 5,318/k_{\rho R_{m=0}} = 12.289\,\mu\mathrm{m}$ (that is where the function $J_4(k_{\rho R_{m=0}}\rho)$ assumes its maximum value).

We can see in Fig. 2(a) the resulting intensity field in a three-dimensional pattern. Its orthogonal projection, shown in Fig. 2(b), clearly confirms the cylindrical surface of light intensity. Figure 3 depicts the transverse intensity pattern at $z = L/2$. It is possible to note that the transverse peak intensity is located at $\rho = 12.285\,\mu\mathrm{m}$, a value near the predicted one. This interesting field configuration is resistant to the attenuation and diffraction effects until the distance $z = 25\,\mathrm{cm}$. We should remember that any other ordinary beam propagating in the same medium at the same frequency would have a penetration depth of only 5 cm.

5. Finite-Aperture Generation of Diffraction–Attenuation Resistant Beams

As we have seen, the solution in Eq. (5), with Eqs. (8), (9), (11), (6), and (13), represents propagating beams in absorbing media with the remarkable characteristic of allowing us to choose the desired LIP on $\rho = 0$, within $0 \le z \le L$, with the spot sizes regulated by the values of the parameter Q. The same occurs with solution in Eq. (31), which in turn allows us to choose the desired LIP on a cylindrical surface.

Now, we must remember that although the beams of Eqs. (5) and (31) are exact solutions, they do not represent beams generated or truncated by finite apertures. Actually, the fields given by these solutions *in all points of space* would require infinite apertures to be generated.

If a Bessel beam given by Eq. (2) is truncated by a finite aperture of radius $R \gg 2.4/k_{\rho R}$ situated on the plane $z = 0$, the radiated field—in the spatial region $0 < z < R/\tan\theta \equiv Z$ (the diffractionless distance of a truncated Bessel beam) and $0 \le \rho \le (1 - z/Z)R$—can be approximately described [2,3,6,42] by Eq. (2).

Taking into account that the solution in Eq. (10) is a linear superposition of Bessel beams, we can expect that, when it is truncated by a finite aperture of

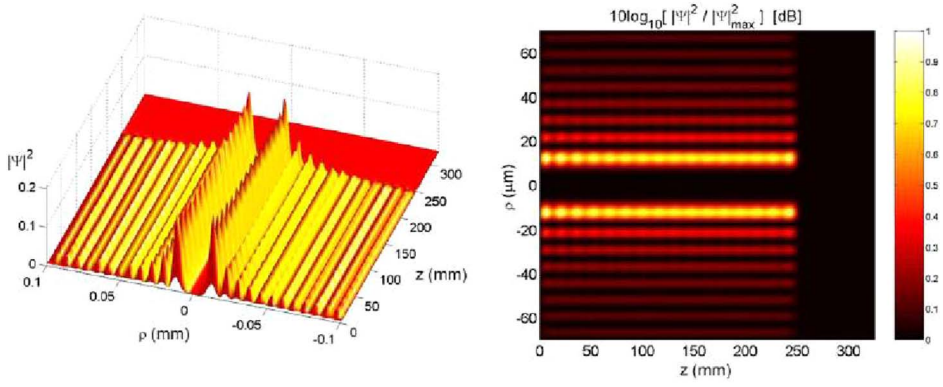

(a) (b)

Fig. 2. (Color online) (a) Three-dimensional field intensity of the resulting beam and (b) its orthogonal projection.

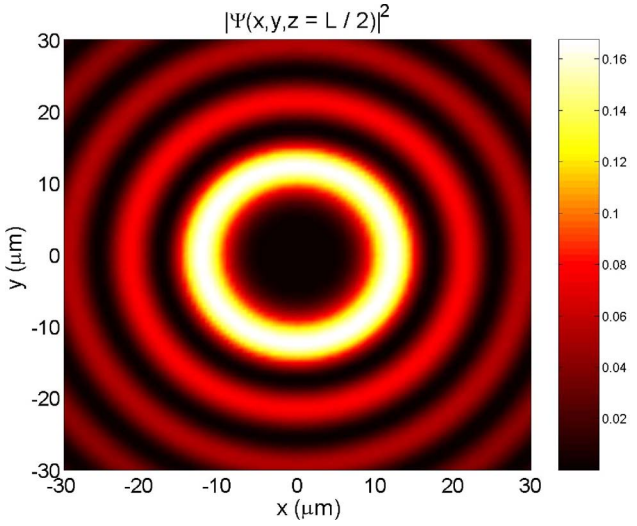

Fig. 3. (Color online) Beam's transverse intensity pattern at $z = L/2$.

radius [43] $R \gg 2.4/k_{\rho R_{m=N}}$, the radiated field in the region [44] $0 < z < R/\tan\theta_{m=-N} \equiv Z_{m=-N}$ and $0 \le \rho \le (1 - z/Z_{m=-N})R$ will be approximately given by Eq. (10).

Now, as we are interested in controlling the LIP of the truncated beam within $0 \le z \le L$, we have to guarantee that all Bessel beams in Eq. (10) maintain their characteristics until $z = L$ after the truncation. This is possible if the following two conditions are satisfied [45]:

$$R \gg \frac{2.4}{k_{\rho R_{m=N}}}, \tag{33}$$

$$Z_{m=-N} > L \rightarrow \frac{R}{\tan\theta_{m=-N}} > L \rightarrow R > L\sqrt{\frac{n_R^2}{c^2}\frac{\omega^2}{\beta_{R_{m=-N}}^2} - 1}. \tag{34}$$

So we can expect that, by choosing a finite aperture of radius R large enough to satisfy Eqs. (33) and (34), the truncated versions of the diffraction–attenuation resistant beams will maintain their characteristics, i.e., we will continue to be able to control the beam's LIP. To confirm our expectation, examples shall be presented below, where we choose desired LIPs and obtain the corresponding ideal beam solutions, $\Psi(\rho,\phi,z,t)$, through Eqs. (5), (8), (9), (11), (6), and (13). These ideal solutions, in turn, are used to obtain their truncated versions, $\Psi_T(\rho,\phi,z,t)$, through numerical calculation of the Rayleigh–Sommerfeld diffraction integral for monochromatic waves [46], namely,

$$\Psi_T(\rho,\phi,z,t) = \frac{1}{2\pi}\int_0^{2\pi} d\phi' \int_0^R d\rho'\rho' \frac{e^{ikD}}{D} \times \left(\frac{\partial}{\partial z'}\Psi(\rho',\phi',z',t)\right)_{z'=0}, \tag{35}$$

where a circular aperture of radius R, on the plane $z' = 0$, is used for the truncation, and $D = \sqrt{(z-z')^2 + \rho^2 + \rho'^2 - 2\rho\rho'\cos(\phi - \phi')}$ is the separation distance between the source and the observation points.

A. First Example

Here, we are going to calculate numerically the truncated version of the ideal diffraction–attenuation resistant beam obtained in the example of Section 2 and in [3].

The medium in question has refractive index $n = n_R + in_I = 1.5 + i0.49 \times 10^{-6}$ for $\lambda = 308\,\text{nm}$ (i.e., $\omega = 6.12 \times 10^{15}\,\text{Hz}$). The ideal beam in that example was constructed to possess (for $\omega = 6.12 \times 10^{15}\,\text{Hz}$) a spot radius $\Delta\rho = 5.6\,\mu\text{m}$ and a constant intensity of its central spot until a distance of 25 cm. These characteristics were reached through the fundamental ideal solution of Eq. (10), with Eqs. (8), (9), (11), (6), and (13), by choosing the desired LIP $|F(z)|^2$ (on $\rho = 0$), within $0 \le z \le L$, according to Eq. (15), putting $Z = 25\,\text{cm}$ and $L = 33\,\text{cm}$. The values of Q and N were chosen to be $0.9999 n_R\omega/c$ and 20, respectively. This ideal beam solution is used as the aperture excitation, $\Psi(\rho',z',t)$, in the Rayleigh–Sommerfeld diffraction integral, Eq. (35), which is numerically calculated to yield $\Psi_T(\rho,z,t)$, i.e., the truncated version of this beam.

According to our discussion above, the truncated beam shall possess a behavior very similar to the ideal one provided that the aperture radius R satisfies the conditions in Eqs. (33) and (34), which furnish, in this case $R \ge 4.9\,\text{mm}$. However, due to the fact that the chosen on-axis LIP has null value within $Z < z < L$, we can replace L in the condition of Eq. (34) with Z, obtaining in this case $R \ge 3.8\,\text{mm}$. We choose $R = 3.8\,\text{mm}$. After numerical calculation of Eq. (35), we obtain the result plotted in Fig. 4. Comparing Fig. 4 with Fig. 1(a) of the ideal beam of Section 2, we can see that our expectations were correct, i.e., by choosing an aperture radius big enough, the truncated version becomes very close to the ideal solution in the spatial region of interest.

B. Second Example

In [3], Zamboni-Rached obtained, in an absorbing medium, an ideal (i.e., not truncated) beam presenting an interesting and counterintuitive characteristic. There, a medium was considered with refractive index $n = n_R + in_I = 1.5 + i0.46 \times 10^{-6}$ (which implies a penetration depth of 5 cm) at $\omega = 6.12 \times 10^{15}\,\text{Hz}$. At this angular frequency, an ideal beam was shaped to possess a spot radius $\Delta\rho = 5.6\,\mu\text{m}$ and a modest exponential growth of its intensity until a distance of 25 cm, suffering after this a strong intensity fall. To reach these characteristics, the desired on-axis LIP, $|F(z)|^2$, within $0 \le z \le L$, was chosen according to

$$F(z) = \begin{cases} \exp(z/Z) & \text{for } 0 \le z \le Z \\ 0 & \text{elsewhere} \end{cases}, \tag{36}$$

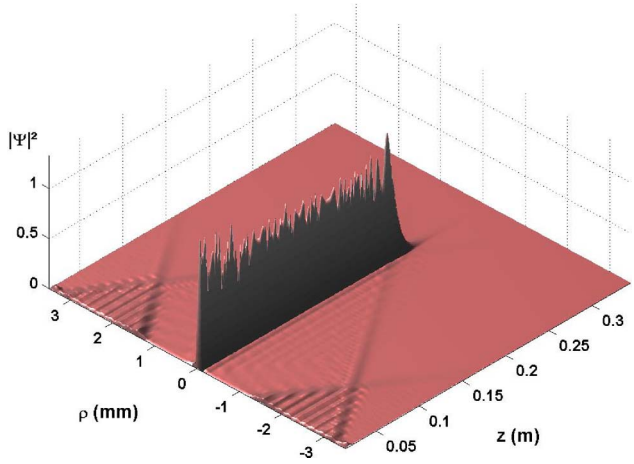

Fig. 4. (Color online) Truncated version of the ideal diffraction–attenuation resistant beam obtained in the example of Section 2.

with $Z = 25\,\text{cm}$ and $L = 33\,\text{cm}$. Taking into account Eq. (14), $Q = 0.9999 n_R \omega/c$ and the value of N was chosen to be $N = 20$.

With this, the (ideal) desired beam, $\Psi(\rho, z, t)$ was obtained in [3] through the fundamental solution in Eq. (10), with Eqs. (8), (9), (11), (6), and (13). The resulting ideal (i.e., not truncated) beam is plotted in Fig. 5.

In this example, we are going to use Eq. (35) to obtain the truncated version, $\Psi_T(\rho, z, t)$, of the above ideal beam. By using the conditions in Eqs. (33) and (34) for efficient finite-aperture generation, we obtain that the aperture radius should obey the condition $R \geq 4.9\,\text{mm}$. But, for the same reason as in the previous example, we can adopt $R \geq 3.8\,\text{mm}$, and we choose $R = 3.8\,\text{mm}$. The numerical calculation of Eq. (35) yields the truncated beam plotted in Fig. 6. We can see an excellent agreement between the ideal beam and the truncated one in the region of interest, confirming that the method works very well in more realistic situations close to the experimental ones.

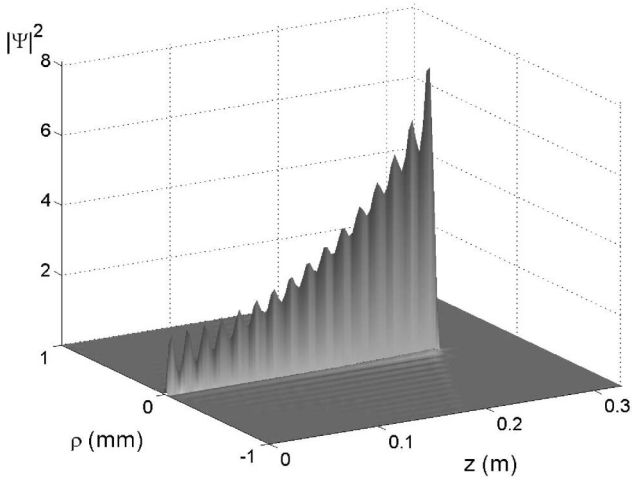

Fig. 5. Ideal beam presenting a moderate exponential growth in an absorbing medium.

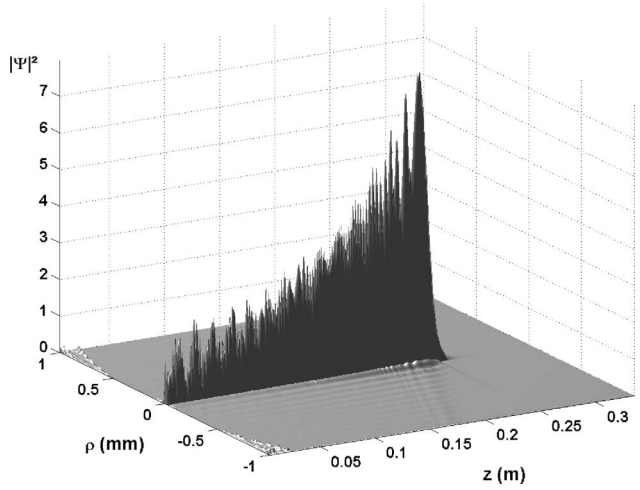

Fig. 6. Truncated version of the beam with exponential growth.

6. Conclusions

A few years ago [3], an interesting theoretical method was developed that allowed the construction, in absorbing media, of axially symmetric beams whose longitudinal intensity pattern (LIP) can be chosen in advance. As a particular case, diffraction–attenuation resistant beams were obtained, that is, beams capable of maintaining both the size and the intensity of their central spots. In this paper, we have elucidated how to apply this scalar method to paraxial electromagnetic waves and extended it to include nonaxially symmetric beams, allowing in this way, besides strong control over the longitudinal intensity pattern, a certain amount of control over the transverse one. With this extension, it is possible to model the LIP of the beams over cylindrical surfaces. In particular, we can construct (in absorbing media) hollow beams resistant to attenuation and diffraction effects.

We have also used the Rayleigh–Sommerfeld diffraction integral to obtain truncated versions of these new beams, verifying that the truncated beams possess the same interesting characteristics of the ideal beams provided, that the aperture used for truncation is big enough. Such a verification is important because it confirms that the method works very well in more realistic situations close to the experimental ones. These new beams have many potential applications, such as in free-space optics, medical apparatus, remote sensing, and optical tweezers.

The authors are grateful, for collaboration and many stimulating discussions over the last few years, to Erasmo Recami. The authors acknowledge the financial support of the National Counsel of Technological and Scientific Development (CNPq) and the State of Sao Paulo Research Foundation (FAPESP) under contracts 2005/51689-2 (CePOF, Optics and Photonics Research Center) and 2009/54494-9 (postdoctoral sponsorship granted to L. A. Ambrosio). They are also indebted to CNPq-FAPESP Instituto Nacional de Ciência e Tecnologia Fotônica para Comunicações Ópticas for their financial support.

References and Notes

1. M. Zamboni-Rached, "Stationary optical wave fields with arbitrary longitudinal shape by superposing equal frequency Bessel beams: Frozen Waves," Opt. Express **12**, 4001–4006 (2004).
2. M. Zamboni-Rached, E. Recami, and H. E. Hernández-Figueroa, "Theory of frozen waves: modeling the shape of stationary wave fields," J. Opt. Soc. Am. A **22**, 2465–2475 (2005).
3. M. Zamboni-Rached, "Diffraction–attenuation resistant beams in absorbing media," Opt. Express **14**, 1804–1809 (2006).
4. H. E. Hernández-Figueroa, M. Zamboni-Rached, and E. Recami, eds., *Localized Waves: Theory and Applications*, (Wiley, 2008), and references therein.
5. C. J. R. Sheppard and T. Wilson, "Gaussian-beam theory of lenses with annular aperture," IEE J. Microwaves Opt. Acoust. **2**, 105–112 (1978).
6. J. Durnin, J. J. Miceli, and J. H. Eberly, "Diffraction-free beams," Phys. Rev. Lett. **58**, 1499–1501 (1987).
7. I. M. Besieris, A. M. Shaarawi, and R. W. Ziolkowski, "A bidirectional traveling plane wave representation of exact solutions of the scalar wave equation," J. Math. Phys. **30**, 1254–1269 (1989).
8. R. W. Ziolkowski, I. M. Besieris, and A. M. Shaarawi, "Aperture realizations of exact solutions to homogeneous-wave equations," J. Opt. Soc. Am. A **10**, 75–87 (1993).
9. J.-Y. Lu and J. F. Greenleaf, "Nondiffracting x-waves: exact solutions to free-space scalar wave equation and their finite aperture realizations," IEEE Trans. Ultrason. Ferroelectr. Freq. Control **39**, 19–31 (1992).
10. E. Recami, "On localized x-shaped superluminal solutions to Maxwell equations," Physica A (Amsterdam) **252**, 586–610 (1998).
11. P. Saari and K. Reivelt, "Evidence of x-shaped propagation-invariant localized light waves," Phys. Rev. Lett. **79**, 4135–4138 (1997).
12. D. Mugnai, A. Ranfagni, and R. Ruggeri, "Observation of superluminal behaviors in wave propagation," Phys. Rev. Lett. **84**, 4830–4833 (2000). This paper aroused some criticisms, to which the authors replied.
13. M. Zamboni-Rached, E. Recami, and H. E. Hernández-Figueroa, "New localized Superluminal solutions to the wave equations with finite total energies and arbitrary frequencies," Eur. Phys. J. D **21**, 217–228 (2002).
14. M. Zamboni-Rached, K. Z. Nóbrega, C. A. Dartora, and H. E. Hernández-Figueroa, "On the localized superluminal solutions to the Maxwell equations," IEEE J. Sel. Top. Quantum Electron. **9**, 59–73 (2003), and references therein.
15. C. Conti, S. Trillo, G. Valiulis, A. Piskarskas, O. Jedrkiewicz, J. Trull, and P. Di Trapani, "Nonlinear electromagnetic x-waves," Phys. Rev. Lett. **90**, 170406 (2003).
16. M. Zamboni-Rached and H. E. Hernández-Figueroa, "A rigorous analysis of localized wave propagation in optical fibers," Opt. Commun. **191**, 49–54 (2001).
17. M. Zamboni-Rached, E. Recami, and F. Fontana, "Localized superluminal solutions to Maxwell equations propagating along a normal-sized waveguide," Phys. Rev. E **64**, 066603 (2001).
18. M. Zamboni-Rached, K. Z. Nóbrega, E. Recami, and F. H. E. Hernandez, "Superluminal x-shaped beams propagating without distortion along a coaxial guide," Phys. Rev. E **66**, 046617 (2002).
19. M. Zamboni-Rached, F. Fontana, and E. Recami, "Superluminal localized solutions to Maxwell equations propagating along a waveguide: the finite-energy case," Phys. Rev. E **67**, 036620 (2003).
20. S. V. Kukhlevsky and M. Mechler, "Diffraction-free subwavelength beam optics at nanometer scale," Opt. Commun. **231**, 35–43 (2004).
21. M. Zamboni-Rached, K. Z. Nóbrega, H. E. Hernández-Figueroa, and E. Recami, "Localized superluminal solutions to the wave equation in (vacuum or) dispersive media, for arbitrary frequencies and with adjustable bandwidth," Opt. Commun. **226**, 15–23 (2003).
22. S. Longhi and D. Janner, "X-shaped waves in photonic crystals," Phys. Rev. B **70**, 235123 (2004).
23. M. Zamboni-Rached and E. Recami, "Subluminal wave bullets: exact localized subluminal solutions to the wave equations," Phys. Rev. A **77**, 033824 (2008).
24. M. A. Porras, R. Borghi, and M. Santarsiero, "Suppression of dispersion broadening of light pulses with Bessel–Gauss beams," Opt. Commun. **206**, 235–241 (2002).
25. M. Zamboni-Rached, H. E. Hernández-Figueroa, and E. Recami, "Chirped optical X-shaped pulses in material media," J. Opt. Soc. Am. A **21**, 2455–2463 (2004).
26. Z. Bouchal and J. Wagner, "Self-reconstruction effect in free propagation wavefield," Opt. Commun. **176**, 299–307 (2000).
27. R. Grunwald, U. Griebner, U. Neumann, and V. Kebbel, "Self-reconstruction of ultrashort-pulse Bessel-like x-waves," in *Conference on Lasers and Electro-Optics / Quantum Electronics and Laser Science Conference* (Optical Society of America, 2004), paper CMQ7.
28. M. Zamboni-Rached, A. Shaarawi, and E. Recami, "Focused x-shaped pulses," J. Opt. Soc. Am. A **21**, 1564–1574 (2004), and references therein.
29. C. J. R. Sheppard and P. Saari, "Lommel pulses: an analytic form for localized waves of the focus wave mode type with bandlimited spectrum," Opt. Express **16**, 150–160 (2008).
30. M. Zamboni-Rached, "Unidirectional decomposition method for obtaining exact localized wave solutions totally free of backward components," Phys. Rev. A **79**, 013816 (2009).
31. When generated by a finite aperture of radius $R \gg 2.4/k_{\rho R}$ situated on the plane $z = 0$, the solution in Eq. (2) becomes a valid approximation only in the spatial region $0 < z < R/\tan\theta \equiv Z$ and to $\rho < (1 - z/Z)R$.
32. In this paper we use cylindrical coordinates (ρ, ϕ, z).
33. Fortunately, these conditions are satisfied for a great number of situations.
34. The same that was given in [3].
35. In an absorbing medium like this, at a distance of 25 cm, these beams would have their initial field intensity attenuated 148 times.
36. According to Eq. (9), the maximum value allowed for N is 158 and we choose to use $N = 20$ just for simplicity. Of course, by using higher values of N we get better results.
37. The analytic calculation of these coefficients is quite simple in this case and their values are not listed here; we just use them in Eq. (10).
38. In this case, we can consider both $\epsilon_b(\omega)$ and $\sigma(\omega)$ real quantities.
39. J. D. Jackson, *Classical Electrodynamics* (Wiley, 1998).
40. Notice that, according to Section 2, the absorption coefficient of a Bessel beam is $\alpha_\theta = \alpha\cos\theta = 2k_I\cos\theta$. When $\theta \to 0$, the Bessel beam tends to a plane wave and $\alpha_\theta \to \alpha$.
41. The idea developed in this section generalizes that exposed in Section 5 of [2], which was addressed to nonabsorbing media.
42. The same is valid for a truncated higher-order Bessel beam.
43. Notice that $k_{\rho R_{m=N}}$ is the smallest value of all $k_{\rho R_m}$, therefore, if $R \gg 2.4/k_{\rho R_{m=N}} \to R \gg 2.4/k_{\rho R_m}$ for all m.
44. Here, θ_m is the axicon angle of the mth Bessel beam in Eq. (5).
45. That is, the shortest diffractionless distance is larger than the distance L.
46. J. W. Goodman, *Introduction to Fourier Optics* (McGraw-Hill, 1968).